

Measuring direction in the coupling of biological oscillators: A case study for electroreceptors of paddlefish

Jorge Brea

*Center for Neurodynamics, University of Missouri-St. Louis, St. Louis,
Missouri 63121*

David F. Russell

Department of Biological Sciences, Ohio University, Athens, Ohio 45701

Alexander B. Neiman

*Department of Physics and Astronomy, Ohio University, Athens, Ohio 45701
and Quantitative Biology Institute, Ohio University, Athens, Ohio 45701*

(Received 15 February 2006; accepted 7 April 2006; published online 30 June 2006)

Recently developed methods for estimating directionality in the coupling between oscillators were tested on experimental time series data from electroreceptors of paddlefish, because each electroreceptor contains two distinct types of noisy oscillators. One type of oscillator is in the sensory epithelia, and another type is in the terminals of afferent neurons. Based on morphological organization and our previous work, we expected unidirectional coupling, whereby epithelial oscillations synaptically influence the spiking oscillators of afferent neurons. Using directionality analysis we confirmed unidirectional coupling of oscillators embedded in electroreceptors. We studied the performance of directionality algorithms for decreasing length of data. Also, we experimentally varied the strength of oscillator coupling, to test the effect of coupling strength on directionality algorithms. © 2006 American Institute of Physics. [DOI: [10.1063/1.2201466](https://doi.org/10.1063/1.2201466)]

Theoretical methods of nonlinear dynamics have been widely applied in time series analyses of multivariate data from biological systems. In particular, modern synchronization theory provides novel methods to identify and assess the degree of interactions of physiological subsystems from multivariate time series. An interesting and challenging problem is to identify and quantify the direction of interactions. Recently, several numerical methods have been proposed to address this issue. However, biological experiments often yield nonideal time series that are short, noisy, and nonstationary. This poses the problem of reliability of predictions made using directionality methods. Here, we used electroreceptors of paddlefish as a well-defined experimental model to test the performance and robustness of directionality methods. Electroreceptors possess two types of noisy oscillators, coupled through excitatory chemical synapses. Directionality of coupling can be predicted from the morphological structure and from previous experimental physiological studies. We studied the performance of directionality algorithms for the decreasing length of data; we showed that methods based on the reconstruction of the phase dynamics are able to correctly identify directionality for short data segments of 1-2 s or about 30–60 oscillator periods. However, for shorter datasets, the results became statistically insignificant, as tested using a surrogate analysis. We also applied these algorithms to nonstationary data, when the coupling strength between oscillators changed in time, and showed excellent performance of directionality analysis.

I. INTRODUCTION

Interacting (coupled) stochastic nonlinear oscillators are ubiquitous in nature, and form a conceptual framework for studying several dynamical properties in neural processing at different levels of nervous systems. Such interactions result in complex rhythms that may be related to either healthy or pathological situations.¹ How various rhythms interact and influence each other is therefore one of the fundamental questions of neurodynamics. From a data analysis point of view, we often face the following problem: given a complex dynamical system comprised of several subsystems, what can we say about their interactions if all that we can extract from the system are multivariate time series of some observables? Such multivariate data can result from multichannel recording, e.g., with a microelectrode array, or multichannel magnetoencephalography (MEG) or electroencephalography (EEG).

Traditional cross-correlation techniques, such as the coherence function,² mutual information^{3,4} and synchronization indices^{5,6} provide symmetric estimates of the strength of interaction. However, they lack important information about causal relationships in interactions, that is, directionality and asymmetry of coupling. Such information is crucial in unraveling the structure of a system from observation of signals from its several components. The introduction of a time lag in these measures, e.g., simple linear cross-correlation, or time-delayed mutual information, may lead to the wrong conclusions, as these measures can be fooled by periodicities in one of the signals, or by feedback loops in interacting subsystems.^{7,8}

Several approaches were proposed recently to address the issue of causality. Methods based on the concept of generalized chaos synchronization⁹ were developed in Refs. 10–12 and were applied to experimental neurophysiological data. These methods are based on mutual nonlinear predictabilities, or mutual nearest neighbors in the reconstructed phase space of the system. These approaches are similar to the concept of Granger causality,^{13,14} where statistical tests are used to inquire whether the predictability of one time series can be improved by the knowledge of a second signal.

In many cases, particularly in neuroscience, interacting physiological subsystems can be represented by weakly coupled nonlinear oscillators,¹⁵ so that information about the instantaneous phases of oscillators is sufficient to describe their dynamics. Under this assumption, Rosenblum and Pikovsky¹⁶ have proposed a method to assess directionality in coupling based on a reconstruction of the phase dynamics of interacting oscillators. These methods were applied to study age-related changes in the directionality of cardiorespiratory interactions in babies.^{17,18} The same approach was used in Ref. 19 to analyze magnetoencephalography (MEG) and electroencephalography (EEG) data in paced movements in humans. In Ref. 21 directionality estimates were used to analyze two channel epileptic EEG. The methods based on information theory, developed by Schreiber⁷ and Paluš,²⁰ are free from the assumption of specific coupling schemes.

Real biological time series are noisy, nonstationary, and often short. This has prompted test studies on the performance and reliability of directionality methods in numerical simulations with simple models^{21,22} or with electronic circuits.²³ However, directionality methods have not been tested on a well-defined biological system, in which the interacting physiological subsystems are well defined as distinct oscillators, whose rhythmical activities are well expressed, and in which the directionality of interactions is understood from previous morphological and physiological studies. In this paper, we use electroreceptors of paddlefish, a well-defined sensory system comprising two distinct and synaptically coupled oscillators as a test model to study the performance of several approaches for measuring the directionality of coupling. The structure of the paper is as follows: Paddlefish electroreceptors are described in Sec. II. In Sec. III, we discuss methods used to assess the directionality in coupling. In Sec. IV we describe the results of applying a directionality analysis to the spontaneous and externally stimulated activity of electroreceptors.

II. EXPERIMENTAL SYSTEM: ELECTRORECEPTORS OF PADDLEFISH

The electrosensory system of paddlefish presents an accessible and experimentally advantageous biological model for studying nonlinear dynamical phenomena, such as stochastic resonance,²⁴ self-sustained oscillations,^{25–27} synchronization,²⁸ and noise-induced transitions.^{29,30} Electrosensitive organs are mainly distributed on an elongated appendage, called the rostrum, located in front of the head, but also cover the gills. The rostrum acts as an antenna in detecting weak electric fields emitted by zooplankton prey.^{24,31} Thousands of electrosensors are grouped into clus-

ters on the dorsal and ventral sides of the rostrum. A single electroreceptor (ER) system is composed of a cluster of 3–35 skin pores, each leading into a short canal that terminates in a sensory epithelium containing approximately 1000 sensory hair cells.³² The hair cells of the cluster are coupled through excitatory synapses to a few (2–5) “primary afferent” sensory neurons whose axons project to the brain. A striking property of ERs is their spontaneous background oscillatory activity. A detailed study of the spontaneous activity of paddlefish ERs has revealed two distinct types of oscillators embedded into an ER system.²⁶ The population of cells in each sensory epithelium generates noisy oscillations at a fundamental frequency $f_e = 26 \pm 1.6$ Hz for different ERs in different fish at room temperature (22 °C).²⁶ These oscillations are represented by continuous extracellular voltage signals, $e(t)$, recorded from ER canals. Grouping together a given ER’s 3–35 sensory epithelia, each with independent oscillators, we term this the “epithelial oscillator” (EO).

According to our current understanding, the EO is unidirectionally coupled to (i.e., synaptically excites) another oscillator, residing in each afferent’s terminal, and driving neuronal spikes. We term this the “afferent oscillator” (AO). Dynamical AO properties can be analyzed from a spike train recorded extracellularly from an afferent axon. In contrast to the EO, the fundamental frequency of the AO, f_a , is distributed over a wide range of 30 to 70 Hz for different afferents in different fish. The unidirectional coupling of the two types of oscillators results in quasiperiodic spontaneous firing patterns of afferent neurons. The structure of power spectra, and of serial correlations of interspike intervals, are determined by the ratio of fundamental frequencies of the EO and the AO, $w = f_e/f_a$,²⁷ which is 0.49 ± 0.08 , estimated from 67 afferents.²⁶ Thus, the two types of oscillators embedded into an ER system operate near the 1:2 mode locking regime. However, they are not synchronized under normal conditions.

Details of the experimental procedures can be found in Ref. 26. Recordings of spontaneous activity were done *in vivo*. Stable extracellular single unit recordings from the cell bodies of afferents were obtained using a tungsten microelectrode advanced into the ganglion of an anterior lateral line nerve. Recordings of epithelial oscillatory potentials were made by advancing a glass pipette electrode into a canal opening. Spikes and canal signals were digitized at 20 and 5 kHz, respectively, using an interface and Spike2 software from Cambridge Electronic Devices. All data processing was done offline. Spike times were identified using Spike2 software. Canal signals were bandpass filtered (10 to 40 Hz) to remove low-frequency trends and high-frequency noise.

A set of bivariate data recorded from an ER is represented by a time series having different structures: a time series of canal oscillations is a continuous stochastic process, $e(t)$, whereas an afferent spike train is represented by a stochastic point process of spike times, $\{\tau_k\}$, $k = 1, \dots, M$, where M is the number of spikes in a recording. Linear analyses of these time series include power spectra of the EO and the AO, $G_{ee}(f)$, $G_{aa}(f)$, along with the coherence function, $\gamma^2(f) = |G_{ae}(f)|^2 / [G_{aa}(f)G_{ee}(f)]$.^{2,33} An example of power spectra of the EO and AO and the coherence function be-

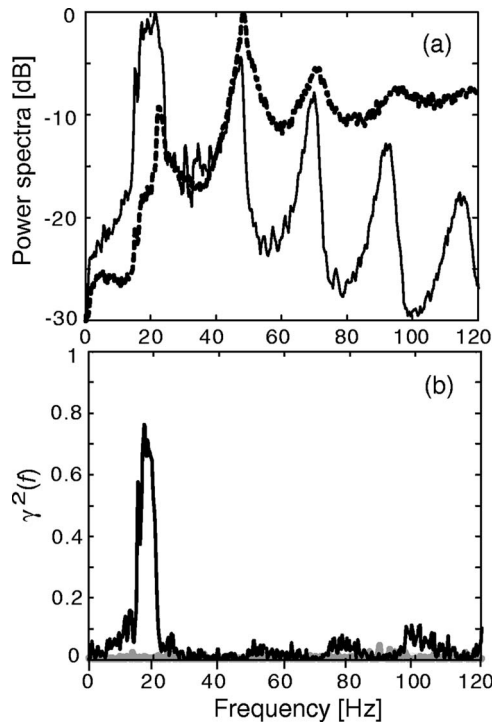


FIG. 1. (a) The power spectra of canal oscillations (solid line) and of an afferent spike train (dashed line). (b) Coherence function calculated between the afferent spike train and the canal oscillations. The coherence function of surrogate data in which afferent spikes were shuffled is shown by the gray line.

tween AO and EO are shown in Fig. 1. The EO power spectrum [Fig. 1(a), solid line] has peaks at the fundamental frequency f_e (approximately 23 Hz in this example) and its higher harmonics. The highest peak in the power spectrum of the AO [Fig. 1(a), dashed line], f_a , corresponds to the mean firing frequency of the afferent neuron, approximately 47 Hz here. Sidebands, $f_a \pm f_e$, are due to excitatory input from the EO. In this example, $w = f_e/f_a \approx 0.5$. The coherence function shows high coherence at the frequency of the EO. However, for some ERs the coherence function also showed a smaller coherence peak at the frequency of the AO, f_a (see, for example, Fig. 2 in Ref. 25), along with minor peaks in the EO power spectrum (see, for example, Figs. 2 and 12 in Ref. 26). These were attributed to the attenuated afferent spikes in canal signals,²⁶ which arise presumably due to proximity of epithelia to afferent terminals undergoing action potentials, which thus may potentially create information flow from the AO to EO. A drawback of the coherence function is that it discards information about instantaneous phases of the EO and AO, which is crucial in determining directionality in their interactions.

To study the phase relations of the two types of ER oscillators, we estimated their instantaneous phases as follows. The phase of an afferent neuron was calculated from its spike times,⁵ τ_k ,

$$\phi_1(t) = 2\pi \frac{t - \tau_k}{\tau_{k+1} - \tau_k} + 2\pi k, \quad \tau_k < t < \tau_{k+1}, \quad (1)$$

that is, the phase of afferent neurons increases by 2π every time a spike occurs and interpolates linearly between two

sequential spikes. A similar approach was used in Ref. 18 for calculation of instantaneous phase from a sequence of R-R intervals of electrocardiograms. The instantaneous phase of the EO was calculated using the analytic signal approach:⁵ an analytic signal $z(t)$ was constructed as a sum of the original canal signal, $e(t)$ and its Hilbert transform: $z(t) = e(t) + e_H(t)$. Then the instantaneous phase of the EO, $\phi_2(t)$, was calculated as the argument of $z(t)$, that is, $z(t) = A(t)\exp[-i\phi_2(t)]$, where $A(t)$ is the instantaneous amplitude of the EO oscillations. The phases $\phi_{1,2}(t)$ will be used as observables for the directionality analysis in the next section.

The phase dynamics of electroreceptors can also be analyzed using a stroboscopic mapping^{26,27} where the phase of the EO, $\phi_2(t)$ is measured at spike times of afferent neuron, τ_k . The probability distribution of the relative phase $\phi_2(\tau_k)$ serves as a measure of timing relation of afferent spikes to canal oscillations. An example of such distribution is given in Fig. 12 of Ref. 26. Although the relative phase distribution was significantly different from a uniform, corresponding synchronization index was very small (< 0.1 for the datasets used here), indicating weak coupling between oscillators. We have shown recently²⁷ that generic phase models accurately describe spontaneous dynamics and statistical properties of paddlefish electroreceptors.

III. METHODS FOR DETECTION OF DIRECTIONALITY

In this study, we used three methods to assess directionality in the interactions of the epithelial and afferent subsystems of electroreceptors. The first and second methods are based on the reconstruction of dynamical equations for phases, as proposed in Refs. 16 and 17, while the third method is based on the information theoretical approach of Refs. 7, 20, and 34. For all methods, we used as observables the EO and AO phases.

If two interacting subsystems can be represented as weakly coupled self-sustained oscillators, then the essence of their dynamics can be captured by just their phases, $\phi_{1,2}$, and an adequate model can be written in the form

$$\dot{\phi}_{1,2} = \omega_{1,2} + f_{1,2}(\phi_1, \phi_2) + \xi_{1,2}(t), \quad (2)$$

where $\omega_{1,2}$ are the natural frequencies of the oscillators, $f_{1,2}(\phi_1, \phi_2)$ are some 2π -periodic coupling functions, and $\xi_{1,2}(t)$ represents noise in the system. Then, if instantaneous phases of oscillators are calculated from the experimental time series, we can reconstruct the coupling functions $f_{1,2}$ and thus estimate how one oscillator influence another.¹⁶

A. Evolution map approach (EMA)

Given two time series of phases, $\{\phi_1(t_k)\}_{k=1}^N$ and $\{\phi_2(t_k)\}_{k=1}^N$ sampled at times $t_k = \Delta t k$, we construct the phase increments,

$$\Delta_{1,2}(t_k) \equiv \phi_{1,2}(t_k + \tau) - \phi_{1,2}(t_k), \quad (3)$$

where τ is a fixed time interval. These increments can be considered as generated by a difference equation,

$$\Delta_{1,2}(t_k) = \omega_{1,2}\tau + F_{1,2}[\phi_{1,2}(t_k), \phi_{2,1}(t_k)] + \eta_{1,2}(t_k), \quad (4)$$

where $F_{1,2}(\phi_1, \phi_2)$ are some unknown functions and $\eta_{1,2}$ are noise sources. The deterministic parts of this equation can be estimated from the phases and the phase increments, as follows: the dependencies of $\Delta_{1,2}$ vs ϕ_1 and ϕ_2 are fitted using the least square method with a finite Fourier series for fitting functions, $\bar{F}_{1,2}(\phi_1, \phi_2) = \sum_{m,l} A_{m,l} e^{im\phi_1 + il\phi_2}$. In the following calculations, the number of Fourier harmonics was truncated to take into account terms with $|l| \leq 3$, $|m| \leq 3$ for $m=0$, $l=0$, and $|m|=|l|=1$ as in Ref. 16.

The measures of the cross dependences of phase dynamics are then calculated using the smooth functions $\bar{F}_{1,2}$ as

$$C_{1,2} = \int_0^{2\pi} \int_0^{2\pi} \left(\frac{\partial \bar{F}_{1,2}}{\partial \phi_{2,1}} \right)^2 d\phi_1 d\phi_2. \quad (5)$$

The cross-coupling index $C_1 > 0$ indicates that the dynamics of ϕ_1 are causally affected by the dynamics of ϕ_2 ; an analogous argument holds for C_2 . We can now define an overall *directionality index* as a normalized difference between these two indices:

$$D = \frac{C_2 - C_1}{C_2 + C_1}. \quad (6)$$

The directionality index varies from 1, if oscillator 1 drives oscillator 2 ($1 \rightarrow 2$), to -1 if oscillator 2 drives oscillator 1 ($2 \rightarrow 1$). These limiting cases correspond to *unidirectional coupling* (in opposite directions). If $D \approx 0$, both oscillators are driving each other, indicating symmetric *bidirectional coupling*. Notice that this index is not well defined if $C_1 + C_2 \approx 0$. We thus need to check for coupling between oscillators by means of other measures such as synchronization indices or the coherence function. It is worth noting that according to this method the cross-coupling indices $C_{1,2}$ and the directionality index D are not affected by asymmetry in the natural frequencies of two oscillators, since $C_{1,2}$ depend only on the first derivative of their corresponding vector fields, and the natural frequencies appear only as an additive constant for $f_{1,2}$. Several studies have addressed the performance of the EMA using numerical simulations and analytical estimates.^{16,17,21,22,35} Modified estimators for the cross-coupling indices were introduced in Ref. 35. In this study, we use the original versions of the EMA described in Ref. 16.

B. Instantaneous period approach (IPA)

The EMA method is not parameter-free, since it includes the time interval τ for calculations of increments. In Ref. 17, an alternative parameter-free method was proposed based on calculations of instantaneous periods. In this method, instantaneous periods $T_{1,2}$ for both oscillators are calculated as the time needed for the phases $\phi_{1,2}(t_k)$ to increase by 2π . In the case of coupled oscillators, the instantaneous periods depend on the states of each oscillator, and can be written as

$$T_{1,2}(k) = \bar{T}_{1,2} + \Phi_{1,2}[\phi_1(t_k), \phi_2(t_k)] + \eta_{1,2}(t_k), \quad (7)$$

where $\bar{T}_{1,2}$ are the mean periods, $\Phi(\phi_1, \phi_2)$ are 2π -periodic unknown functions, and $\eta_{1,2}(t_k)$ are noise sources. As in the

EMA method, the deterministic component $\Phi_{1,2}$ is calculated by least squares fitting with a Fourier series. The cross-coupling indices $C_{1,2}$ are then calculated using Eq. (5) with the appropriate smooth functions, $\bar{\Phi}_{1,2}$, obtained from least squares fitting. Similarly, the directionality index is calculated according to Eq. (6). Unlike the EMA, the cross-coupling indices and the directionality index of the IPA depend on the natural frequencies of oscillators.¹⁷

For a good fitting, both the EMA and IPA methods require the trajectories in phase space of ϕ_1 and ϕ_2 to fill a torus. This imposes a requirement on the length of datasets, but also implies that the oscillators are not synchronized.¹⁶

C. Information theoretic approach (ITA)

The two methods described previously are in line with a general trend known as structural equation modeling. A fundamental drawback of these methods, when they are extended to include nonlinear equations, is the lack of any systematic way to choose an appropriate model for fitting the vector fields. Methods based on information theory are free from assumptions of any particular model.

Let $\{X(t_k)\}_{k=1}^N$ and $\{Y(t_k)\}_{k=1}^N$ be two time series measured from a system. We consider these time series as realizations of Markovian processes, $X(t)$ and $Y(t)$, which can be characterized by a set of conditional probabilities. For example, $P(x_{t_{k+1}} | x_{t_k}^n; y_{t_k}^m)$ denotes the probability to find X with a value $x_{t_{k+1}}$ at t_{k+1} conditioned to the previous n values of X and m values of Y : $x_{t_k}^n = (x_{t_k}, x_{t_{k-1}}, \dots, x_{t_{k-n}})$, $y_{t_k}^m = (y_{t_k}, y_{t_{k-1}}, \dots, y_{t_{k-m}})$. If these two processes are independent, then

$$P(x_{t_{k+1}} | x_{t_k}^n; y_{t_k}^m) = P(x_{t_{k+1}} | x_{t_k}^n). \quad (8)$$

On the contrary, the equality (8) is violated if $X(t)$ and $Y(t)$ are correlated. In this case, a distance between conditional probabilities can be measured in terms of a Kullback entropy,

$$T_{Y \rightarrow X} = \sum P(x_{t_{k+1}}, x_{t_k}^n, y_{t_k}^m) \log \frac{P(x_{t_{k+1}} | x_{t_k}^n; y_{t_k}^m)}{P(x_{t_{k+1}} | x_{t_k}^n)}. \quad (9)$$

This measure introduced in Ref. 7 was called *transfer entropy*. It characterizes an exchange of information between two subsystems, and is very general. First, notice that it addresses the problem of feedback loops mentioned in the Introduction, since $T_{Y \rightarrow X}$ takes into account past states of the process $x_{t_k}^n$. Second, if we know that a third subsystem $Z(t)$ drives one or both subsystems $X(t)$ and $Y(t)$, we can take this into account by conditioning the probability distributions under the logarithm to $z_{t_k}^l$ for some appropriate l .

In the case of $m=n=1$, the transfer entropy (8) is closely related to the conditional mutual information introduced in Ref. 20:

$$C(y; x_\tau | x) = \sum P(x_{t_k+\tau}, x_{t_k}, y_{t_k}) \log \frac{P(x_{t_k+\tau} | x_{t_k}, y_{t_k})}{P(x_{t_k+\tau} | x_{t_k})}, \quad (10)$$

where τ is a fixed time interval. In Ref. 34, this measure was adapted to the case when two subsystems are represented by interacting oscillators, so that the observables are given by the phases of oscillators $\phi_{1,2}(t)$ and the phase increments (3).

Then the conditional mutual information provides cross-coupling indices $C_{1,2}(\phi_{1,2}; \Delta_{2,1} | \phi_{2,1})$, akin to the EMA method, and the directionality index can be calculated according to Eq. (6). In the calculations below, we use this ITA method to complement the EMA method. Just like EMA, the ITA method includes a parameter τ . However, it is also influenced by the partitioning of the sampled data, necessary for an estimation of probability distributions (see, for discussion, Refs. 8 and 20). In this paper, we follow Ref. 34 and use a box counting algorithm based on equiprobable marginal equiquantization bins.³⁶

IV. DIRECTIONALITY OF INTERACTIONS IN ELECTRORECEPTORS

Our present understanding of the ER structure and physiology, as a system of two coupled self-sustained oscillators, allows us to predict the outcome of directionality analysis: we expect to find strong asymmetry in coupling, showing that the epithelial oscillations influence the firing of afferent neurons. In the following, we use notations C_1 to characterize coupling from the epithelial oscillator to the afferent oscillator, (EO \rightarrow AO), and C_2 for the reverse coupling, AO \rightarrow EO. We expect unidirectional coupling, with C_1 significantly larger than C_2 , and a negative directionality index D , Eq. (6) close to -1 .

As was shown recently,³⁵ the EMA's cross-coupling indices $C_{1,2}$ are biased for short datasets. The bias becomes significant in the case when two analyzed signals have structural differences, such as different amounts of noise and different average frequencies. As a result, false directionality may be detected, even in uncoupled systems. The two oscillators embedded in the ER system have distinct frequencies, different variability, and their phases are estimated by different methods. To address the issue of false directionality detection, we used a simple statistical test by creating surrogates that preserved most of the structural asymmetry of the signals, but destroyed their cross-correlations.³⁴ In particular, we created surrogates for the afferent spike train by repeatedly shuffling the order of interspike intervals, while the EO signal was kept unchanged. This procedure preserves the probability distribution of interspike intervals, and thus the mean frequency and the coefficient of variation, but destroys all serial and cross-correlations. The cross-coupling indices $C_{1,2}$ are then calculated for an ensemble of surrogates and compared with the original data.

For the EMA and the ITA methods, the parameter τ was chosen as 8.33 ms, which is approximately a quarter of the period of the EO, and half the period of the AO. We found no significant differences in cross-coupling indices when this parameter was changed.

Datasets from six different ERs from three different fish were used. To minimize nonstationarity, we used data segments 120–600 s in length, in which a simple moving average of the afferent firing rate over a 10 s window fluctuated less than $\pm 2\%$ from the mean rate for the data.

Figure 2 shows a representative example of cross-coupling indices calculated by three different methods across a 300 s dataset recorded from an electroreceptor. The fundamental frequencies of the EO and the AO, estimated from the

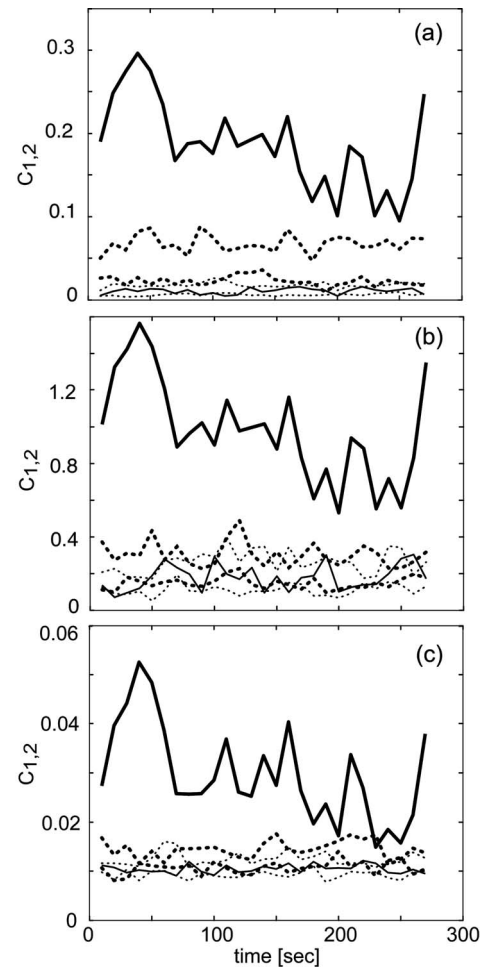


FIG. 2. (a) Cross-coupling indices calculated in a 20 s sliding window for a 300 s dataset using the EMA method. C_1 (EO \rightarrow AO) is shown by the thick solid line. The two thick dotted lines show the maximum and minimum values of C_1 for surrogates. C_2 (AO \rightarrow EO) is shown by the thin solid line; the corresponding maximal and minimal values for surrogates are shown by thin dotted lines. In (b) and (c), the same data were analyzed by the IPA and ITA methods, respectively, and are presented as in (a).

main peaks in their power spectra, were 32 and 77 Hz, respectively. The coherence function reached a maximum value of 0.46 near the fundamental frequency of the EO. The cross-coupling indices $C_{1,2}$ were calculated in a 20 s sliding window with 10 s shift; each time window used for calculations of the cross-coupling indices corresponded to approximately 640 periods of the EO.

In Fig. 2(a) we show the cross-coupling index C_1 (EO \rightarrow AO) and C_2 (AO \rightarrow EO). Unidirectional coupling is obvious from the observation that $C_1 \gg C_2$ throughout the data. Fluctuations in C_1 were presumably due to nonstationarity of the data. An application of the ensemble of ten shuffled surrogates for the afferent spike train demonstrated statistical significance of the estimates C_1 . We clearly see that the values for C_1 , indicating coupling EO \rightarrow AO, for the original data, are significantly higher than those for the surrogate data. On the other hand, the values of C_2 (AO \rightarrow EO) for the original data are within the range of surrogates and thus statistically insignificant, indicating that afferent spikes do not influence epithelial oscillations.

TABLE I. Time-averaged directionality indices for six electroreceptors, calculated in a 20 s sliding window using three different methods. The numbers in brackets are the standard deviations.

ER#	1	2	3	4	5	6
EMA	-0.95 (0.02)	-0.88 (0.05)	-0.89 (0.04)	-0.91 (0.03)	-0.90 (0.03)	-0.90 (0.06)
IPA	-0.80 (0.08)	-0.64 (0.14)	-0.71 (0.11)	-0.77 (0.10)	-0.67 (0.11)	-0.74 (0.14)
ITA	-0.52 (0.18)	-0.52 (0.17)	-0.67 (0.07)	-0.68 (0.07)	-0.57 (0.08)	-0.51 (0.15)

This analysis shows that epithelial oscillations affect the afferent firing. Similar calculations are shown in Figs. 2(b) and 2(c) for two other methods. Both the IPA and the ITA methods showed a successful identification of the directionality of coupling, indicated by C_1 being larger than C_2 throughout the dataset, and by the statistical significance of C_1 estimated from surrogates.

Five other datasets from different electroreceptors, analyzed using the same parameters, showed similar results summarized in Table I, where the directionality index D [Eq. (6)] was averaged over each of the datasets, for each of the three analysis methods. Although all three methods indicated strong asymmetry in coupling, the absolute values of the directionality index were largest for the EMA, which also gave small standard deviations. In contrast, the ITA showed the smallest absolute values for directionality, but the largest standard deviations.

A. Dependence on the time window

We have shown previously that all three algorithms correctly identified the direction of coupling between oscillators, for a rather large sliding window of 20 s, which corresponded to 640 periods of the slower (epithelial) oscillators. However, in many relevant physiological applications, the sizes of datasets can be much smaller. To study finite-size effects of the directionality methods, we partitioned datasets into segments, each of length ΔT . The number of segments L was kept constant, $L=40$, for different segment sizes ΔT . The mean value of the directionality index $D(\Delta T)$ was obtained by averaging over the ensemble of L segments, and its dependence on the size ΔT was calculated. We also studied the size dependence of the coefficient of variation of the directionality index, calculated as the ratio of its standard deviation to the absolute value of its mean,

$$CV(\Delta T) = \frac{\sqrt{\langle D(\Delta T)^2 \rangle - \langle D(\Delta T) \rangle^2}}{|\langle D(\Delta T) \rangle|}, \quad (11)$$

where averaging $\langle \cdot \rangle$ is taken over the ensemble of L segments.

Figure 3(a) shows the mean values of the directionality index for all three methods, as a function of the window size ΔT . As expected, all three methods correctly detected the direction of the coupling for large windows. But, as ΔT decreased, the directionality indices were biased toward smaller values. For the IPA and ITA methods, fluctuations of $D(\Delta T)$ grew rapidly as ΔT decreased [Fig. 3(b)], while the directionality index from the EMA was still significantly negative (-0.76) with small coefficient of variation (<0.2) even for a

1 s window. This demonstrates a significant advantage of the evolution map approach (EMA) for short datasets.

To address the problem of statistical significance of the directionality estimates, we again used the surrogates approach. An ensemble of 40 surrogates for the afferent spike train was constructed for each time window, to test a null hypothesis that the values of cross-coupling indices merely result from biases of the methods due to finite size effects and asymmetries in the signals. The mean value and the standard deviation of cross-coupling indices for the surrogates were calculated and compared to the mean values for the original data, using a well-known measure of statistical significance,^{37,38}

$$K_{1,2}(\Delta T) = \frac{\langle C_{1,2} \rangle - \langle C_{1,2}^{\text{surr}} \rangle}{\sigma^{\text{surr}}}, \quad (12)$$

where K is the statistical significance in units of the standard deviation, $\langle C_{1,2} \rangle$ and $\langle C_{1,2}^{\text{surr}} \rangle$ are the mean value of the cross-couplings indices for the original data and surrogates, respectively, and σ^{surr} is the standard deviation of the surrogate values. Assuming Gaussian statistics, $K \geq 3$ indicates that the null hypothesis can be rejected with confidence greater than 99%.

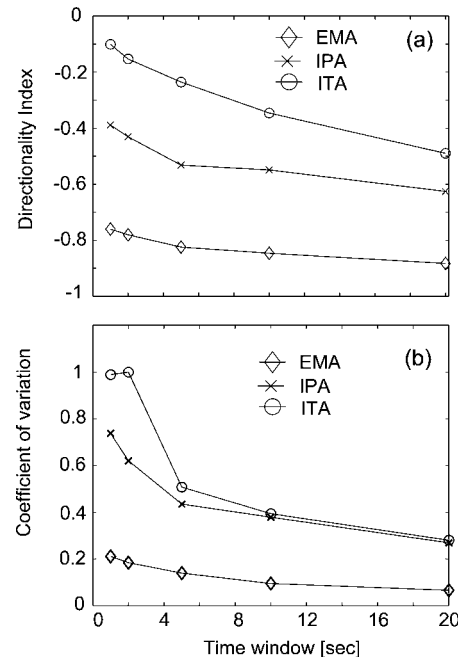


FIG. 3. (a) The average directionality index for the three methods as a function of window size ΔT . (b) Coefficient of variation of the directionality index (11) as a function of ΔT .

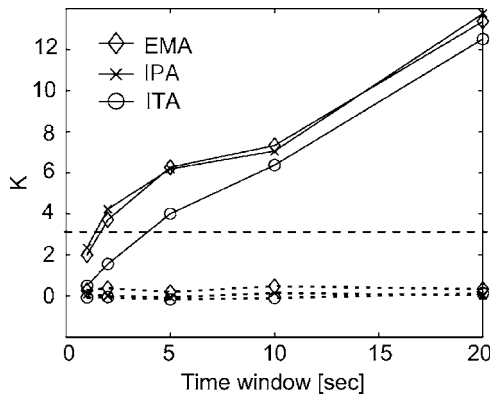


FIG. 4. Statistical significance K for the cross-coupling indices C_1 (EO \rightarrow AO) (solid lines) and C_2 (AO \rightarrow EO) (dotted lines) as a function of the window size. The horizontal dashed line indicates $K=3$ corresponding to 99% of significance level.

The dependence of $K_{1,2}$ versus window size ΔT is shown in Fig. 4. The cross-coupling index C_1 of the EMA and the IPA algorithms showed almost identical behavior, reaching the 99% significance level for short (1.5 s) windows, or approximately 48 periods of the EO. The ITA method, however, required larger windows >4 s to reach this significance level. For the time windows greater than 5 s, all three methods gave statistically significant estimates of C_1 . In contrast, all three methods show no statistical significance for the cross-coupling index C_2 (AO \rightarrow EO), strongly indicating unidirectional coupling from the EO to the AO. Similar results were obtained for other five data sets used in this study.

B. Coupling changing in time

The amplitude of epithelial oscillations can be altered experimentally.²⁵ In such experiments, oscillations in all but one canal in the receptive field of an afferent were inactivated. The one remaining viable canal was stimulated through a recording pipette. Spontaneous canal oscillations became undetectably small after a brief negative stimulus, but then gradually returned over the course of 10 s, as shown in Fig. 5(a). Thus, the instantaneous amplitude of the EO increased in time, which corresponds to an increase of coupling strength to an observed afferent oscillator.

To apply directionality measures to this nonstationary data, we calculated the cross-coupling indices in a 2 s sliding window with 0.5 s shift. The time-dependent cross-coupling indices are shown in Fig. 5(b) for the EMA method. The IPA method gave similar results, but the ITA method was not used because it required larger window size for statistically significant detection of coupling. The EMA's cross-coupling index C_1 followed the amplitude of the EO oscillations, demonstrating excellent performance of the EMA method in reconstructing the coupling scheme.

V. CONCLUSIONS

We have analyzed the performance of three different methods of measuring directionality in coupling, using experimental data from electroreceptors of paddlefish. All three methods were specifically designed for the case of weakly

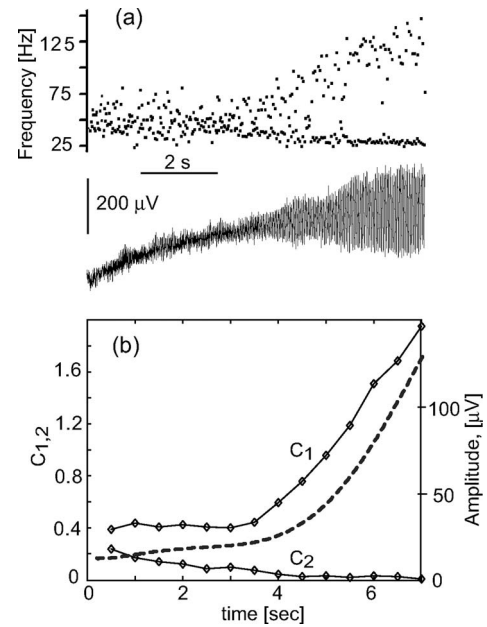


FIG. 5. (a) Instantaneous firing rate of an afferent neuron (upper trace), and canal oscillations (lower panel) of an electroreceptor after stimulating the canal (see the text). (b) Cross-coupling indices $C_{1,2}$ calculated by EMA (solid lines, left vertical axis), and smoothed amplitude of the EO (dashed line, right vertical axis).

coupled nonlinear self-sustained oscillators, where the phases of the oscillators are well defined and used as dynamical variables of interest. Electroreceptors provided an appropriate test model system, as they have two distinct unidirectionally coupled oscillators: epithelial oscillations synaptically coupled to each afferent neuron. We used shuffled surrogates of neuronal spike trains to assess the statistical significance of directionality estimates.

For relatively large datasets (20 s, or more than 640 periods of the slower epithelial oscillator), all three methods showed correct direction in coupling. The evolution map approach showed better results in that the directionality index was closer to -1 and had smaller fluctuations throughout the datasets, compared to the other two methods.

As datasets get shorter, the reliability of these algorithms worsened. Nevertheless, the evolution map approach and the instantaneous period approach showed statistically significant results for datasets as short as 1–2 s, corresponding to 30–60 periods of epithelial oscillations. This is in agreement with the findings of Ref. 17 for cardiorespiratory time series. The ITA method needed larger datasets of >4 s to provide estimates at the same significance level. Excellent performance of the evolution map approach was shown on experimental data when the amplitude of epithelial oscillations evolved in time.

ACKNOWLEDGMENTS

We thank Michael Rosenblum, Kevin Dolan, and Frank Moss for comments and discussions. This work was supported by the U.S. National Institute on Deafness and Other Communication Disorders (DC-04922), and by the U.S. National Science Foundation (INT-0233264). J.B. was also supported by the University of Missouri–Saint Louis Disserta-

tion Year Fellowship and by the U.S. Office of Naval Research.

- ¹L. Glass, *Nature* **410**, 277 (2001).
- ²J. S. Bendat and A. G. Piersol, *Random Data: Analysis and Measurement Procedures*, 3rd ed. (Wiley, New York, 2000).
- ³H. D. I. Abarbanel, *Analysis of Observed Chaotic Data* (Springer-Verlag, New York, 1997).
- ⁴H. Kantz and T. Schreiber, *Nonlinear Time Series Analysis* (Cambridge University Press, Cambridge, 1997).
- ⁵M. G. Rosenblum, A. S. Pikovsky, J. Kurths, C. Schäfer, and P. Tass, "Phase synchronization: From theory to data analysis," in *Handbook of Biological Physics*, Neuro-Informatics and Neural Modeling, edited by F. Moss and S. Gielen (Elsevier Science, Amsterdam, 2001), Vol. 4, Chap. 9, pp. 279–321.
- ⁶A. Pikovsky, M. Rosenblum, and J. Kurths, *Synchronization: A Universal Concept in Nonlinear Science* (Cambridge University Press, Cambridge, 2001).
- ⁷T. Scheiber, *Phys. Rev. Lett.* **85**, 461 (2000).
- ⁸A. Kaiser and T. Schreiber, *Physica D* **166**, 43 (2002).
- ⁹N. F. Rulkov, M. M. Sushchik, and L. S. Tsimring, *Phys. Rev. E* **51**, 980 (1995).
- ¹⁰S. J. Schiff, P. So, and T. Chang, *Phys. Rev. E* **54**, 6708 (1996).
- ¹¹M. L. Van Quyen, J. Martinerie, C. Adam, and F. J. Varela, *Physica D* **127**, 250 (1999).
- ¹²R. Quiñan Quiroga, J. Arnold, and P. Grassberger, *Phys. Rev. E* **61**, 5142 (2000).
- ¹³C. W. J. Granger, *Econometrica* **37**, 424 (1969).
- ¹⁴C. W. J. Granger, *J. Econ. Dyn. Control* **2**, 329 (1980).
- ¹⁵F. C. Hoppensteadt and E. M. Izhikevich, *Weakly Connected Neural Networks* (Springer-Verlag, New York, 1997).
- ¹⁶M. G. Rosenblum and A. Pikovsky, *Phys. Rev. E* **64**, 045202 (2001).
- ¹⁷M. G. Rosenblum, L. Cimponeriu, A. Bezerianos, A. Patzak, and R. Mrowka, *Phys. Rev. E* **65**, 041909 (2002).
- ¹⁸R. Mrowka, L. Cimponeriu, A. Patzak, and M. G. Rosenblum, *Am. J. Physiol.* **285**, R1395 (2003).
- ¹⁹L. Cimponeriu, M. G. Rosenblum, T. Fieseler, J. Dammers, M. Schiek, M. Majtanik, P. Morosan, A. Bezerianos, and P. Tass, *Prog. Theor. Phys. Suppl.* **150**, 22 (2003).
- ²⁰M. Palus, V. Komárek, Z. Hrnčíř, and K. Štěrbová, *Phys. Rev. E* **63**, 046211 (2001).
- ²¹D. A. Smirnov, M. B. Bodrov, J. L. Perez Velazquez, R. A. Wennberg, and B. P. Bezruchko, *Chaos* **15**, 024102 (2005).
- ²²D. A. Smirnov and R. G. Andrzejak, *Phys. Rev. E* **71**, 036207 (2005).
- ²³B. Bezruchko, V. Ponomarenko, M. G. Rosenblum, and A. Pikovsky, *Chaos* **13**, 179 (2003).
- ²⁴D. F. Russell, L. A. Wilkens, and F. Moss, *Nature* **402**, 291 (1999).
- ²⁵A. B. Neiman and D. F. Russell, *Phys. Rev. Lett.* **86**, 3443 (2001).
- ²⁶A. B. Neiman and D. F. Russell, *J. Neurophysiol.* **92**, 492 (2004).
- ²⁷A. B. Neiman and D. F. Russell, *Phys. Rev. E* **71**, 061915 (2005).
- ²⁸A. B. Neiman, X. Pei, D. F. Russell, W. Wojtenek, L. A. Wilkens, F. Moss, H. A. Braun, M. Huber, and K. Voigt, *Phys. Rev. Lett.* **82**, 660 (1999).
- ²⁹A. B. Neiman and D. F. Russell, *Phys. Rev. Lett.* **88**, 138103 (2002).
- ³⁰S. Liepelt, J. A. Freund, L. Schimansky-Geier, A. B. Neiman, and D. F. Russell, *J. Theor. Biol.* **237**, 30 (2005).
- ³¹L. A. Wilkens, D. F. Russell, X. Pei, and C. Gurgens, *Proc. R. Soc. London, Ser. B* **264**, 1723 (1997).
- ³²J. M. Jørgensen, A. Flock, and J. Wersäll, *Z. Zellforsch Mikrosk Anat.* **130**, 362 (1972).
- ³³F. Gabbiani and C. Koch, in *Methods in Neural Modeling: from Ions to Networks*, edited by C. Koch and I. Segev (MIT, Cambridge, MA, 1998), pp. 313–360.
- ³⁴M. Paluš and A. Stefanovska, *Phys. Rev. E* **67**, 055201 (2003).
- ³⁵D. A. Smirnov and B. P. Bezruchko, *Phys. Rev. E* **68**, 046209 (2003).
- ³⁶M. Paluš, *Physica D* **93**, 64 (1996).
- ³⁷J. Theiler, B. Galdrikian, A. Longtin, S. Eubank, and J. D. Farmer, *Physica D* **58**, 77 (1992).
- ³⁸K. Dolan, M. L. Spano, and F. Moss, "Detecting unstable periodic orbits in biological systems," in *Handbook of Biological Physics*, Neuro-Informatics and Neural Modeling, edited by F. Moss and S. Gielen (Elsevier ScienceAmsterdam, 2001), Vol. 4, pp. 131–153.